

BEDT-TTF organic superconductors: the entangled role of phonons

Alessandro Giardino,¹ Matteo Masino,¹ Aldo Brillante,² Rachele G. Della Valle,² and Elisabetta Venuti²¹Dip. di Chimica Gen. Inorg. Chim. Anal. e Chim. Fis. and INSTM - UdR Parma, Parma University, 43100 Parma, Italy²Dip. di Chimica Fisica ed Inorganica and INSTM - UdR Bologna, Bologna University, Bologna, Italy

(Dated: October 18, 2019)

We calculate the lattice phonons and the electron-phonon coupling of the organic superconductor $-(BEDT-TTF)_2I_3$, reproducing all available experimental data connected to phonon dynamics. Low frequency intramolecular vibrations are strongly mixed to lattice phonons. Both acoustic and optical phonons are appreciably coupled to electrons through the modulation of the hopping integrals (e-EP coupling). By comparing the results relevant to superconducting $-\text{and } -(BEDT-TTF)_2I_3$, we show that electron-phonon coupling is fundamental to the pairing mechanism. Both e-EP and electron-molecular vibration (e-MV) couplings are essential to reproduce the critical temperatures. The e-EP coupling is stronger, but e-MV is instrumental to increase the average phonon frequency.

Organic superconductors (oSC) have been studied for more than twenty years, but the nature of the pairing mechanism is still unknown, and remains one of the most intriguing problems in this class of materials [1]. Like high T_c superconductors, oSC are low-dimensional systems characterized by strong electronic correlations. This fact and the proximity of the superconducting phase to magnetically or charge ordered states has brought about the suggestion of exotic pairing, mediated for instance by spin or charge fluctuations [2]. However, direct experimental evidence for such kind of purely electronic mechanisms has not been provided. On the other hand, the oSC phonon structure is very complex, preventing a clear assessment of the role of phonons in the pairing. Indeed, scattered experimental evidences of the involvement of intramolecular phonons [3], of optical intermolecular phonons [4], and of acoustic phonons [5] have been presented. However, all these studies, focusing on a particular type of phonon, failed to offer a comprehensive and convincing picture of the phonon mediated mechanism in oSC. Aim of this letter is to provide a unified framework for the description of the phonon dynamics and of the electron-phonon coupling in oSC based on bisethylenedithio-tetrathiafulvalene (BEDT-TTF). We shall show that all the above types of phonons are coupled to electrons, and cooperate in establishing electron pairing.

In molecular crystals it is convenient to start by distinguishing between intra- and intermolecular vibrational degrees of freedom, and to consider their interactions at a later stage. Thus, in the framework of a tight-binding description of the electrons, intramolecular vibrations modulate the on-site energy and yield the electron-molecular vibration (e-MV) coupling, while lattice phonons, mainly intermolecular in character, modulate the hopping integrals (e-EP coupling).

Molecular vibrations and e-MV coupling constants are transferable among different crystalline phases, and either computational or experimental methods can be used for their determination. Indeed, BEDT-TTF molecular normal modes and e-MV coupling constants are fairly well known [6]. The problem of lattice phonons is much

harder to deal with, because the experimental characterization of lattice phonons and of e-EP coupling constants is difficult and subject to considerable experimental uncertainty [4]. Moreover, the phonon properties are not transferable among different crystals. To overcome these difficulties, we have adopted the "Quasiharmonic Lattice Dynamics" (QHLD) computational method [7, 8], which is known to accurately predict the crystal structure and the phonon dynamics of complex molecular crystals as a function of pressure p , and temperature T .

As extensively discussed elsewhere [7, 8], in QHLD the vibrational contribution to the crystal Gibbs energy $G(p;T)$ is approximated by the free energy of the phonons calculated in the harmonic approximation. The structure at a given p, T is determined self-consistently by minimizing $G(p;T)$ with respect to lattice parameters, molecular positions and orientations. The method relies on an accurate intermolecular potential model, which we have described as the sum of empirical atom-atom potentials, known to be reasonably transferable among crystals containing similar molecules. We have restricted our attention to the $(BEDT-TTF)_2I_3$ salts, which constitute an ideal benchmark for our approach. Our strategy has been to determine and to fix once and for all the needed C, S, H and I atom-atom parameters on the basis of the crystal structures of neutral BEDT-TTF and non-superconducting $-(BEDT-TTF)_2I_3$ salt [8]. We have then applied the method to the phonon structure and e-EP coupling strength of superconducting $-(BEDT-TTF)_2I_3$ salt [7]. Here we illustrate the corresponding results for $-(BEDT-TTF)_2I_3$. The comparison with the experimental data for the two superconducting $-\text{and } -$ phases allows us to validate our approach and to assess the role of phonons in the superconductivity mechanism.

Since both I_3 and BEDT-TTF present low frequency intramolecular modes falling in the region of the lattice phonons, the coupling between inter- and intramolecular phonons may be important for the $(BEDT-TTF)_2I_3$ salts. To account for this effect, we use the exciton-like model described elsewhere [7]. We stress that lattice phonons are actually mixed only with low-frequency vibrations

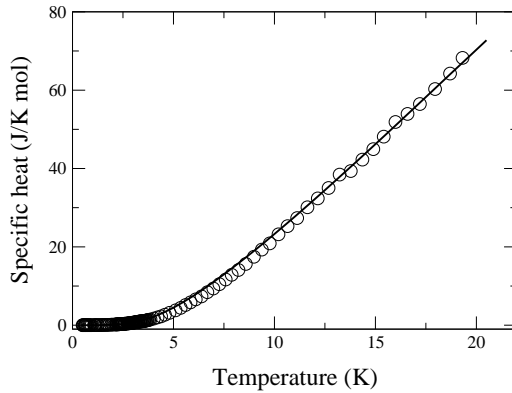


FIG. 1: Calculated (c_v , full line) and experimental (c_p , circles, from Ref. 10) $-(BEDT-TTF)_2I_3$ specific heat.

(below 300 cm^{-1}), and these do not modulate on-site energies [6]. Therefore e-LP and e-MV couplings can be dealt with separately.

At room temperature, $-(BEDT-TTF)_2I_3$ crystallizes in the monoclinic system $P2_1=c$, with four molecules per unit cell. Upon cooling below 150 K the crystal structure changes to the $P2_1$ system [9]. The BEDT-TTF layer is in the bc plane. The QHLD calculations reproduce both crystal structures, which correspond to two distinct $G(p;T)$ minima. The calculated lattice parameters are within 3% of the experimental ones. The results presented below all refer to the low temperature phase.

A comparison with $-(BEDT-TTF)_2I_3$ scanty infrared and Raman data does not offer a stringent test for the calculated phonon frequencies, whose number largely exceeds that of the currently observed bands. We then compare the experimental [10] specific heat c_p to the calculated c_v , which depends on the overall distribution of phonon frequencies ω_{qj} : $c_v(T) = k_B \sum_{qj} F(\hbar \omega_{qj} / k_B T)$, where $F(x) = x^2 e^x (e^x - 1)^2$ and the sum is extended to all phonon branches j and wavevectors q . As shown in Fig. 1, the agreement is outstanding. We stress that there are no adjustable parameters in our $c_v(T)$ calculation.

To calculate the e-LP coupling strength we assume that the low frequency phonons, mainly intermolecular in character, couple to electrons only through the modulation of hopping integrals:

$$t_{KL} = \sum_j t_{KL}^0 + g(KL; qj) Q_{qj} \quad (1)$$

where t_{KL} is the hopping integral between neighboring pairs KL of BEDT-TTF molecules, and Q_{qj} are the dimensionless normal coordinates. Finally, $g(KL; qj) =$

$h=2!_{qj}$ ($t_{KL}^0 = \theta Q_{qj}$) defines the linear e-LP coupling constants. The t_{KL}^0 and their dependence from the QHLD eigenvectors Q_{qj} have been calculated by the extended Hückel (EH) method [7]. The obtained t^0 values are in good agreement with those calculated by extended basis set density functional methods [11]. The t^0 are

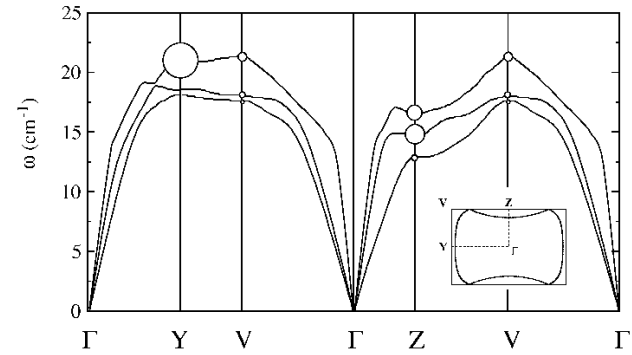


FIG. 2: Dispersion curves of $-(BEDT-TTF)_2I_3$ acoustic lattice phonons along the principal directions shown in the inset. Inset: Fermi surface calculated with the dimer model.

used to describe the band structure in a tight binding approach, adopting the dimer model [12]. The resulting conduction bands and Fermi surface (inset of Fig. 2) match closely those obtained considering all the four site orbitals within the unit cell [9].

To express the e-LP coupling constants in reciprocal space, we have to introduce the dependence on both electronic (k) and phononic (q) wavevectors. We have followed the approximation scheme adopted for $-(BEDT-TTF)_2I_3$ [7]. The k dependence has been accounted for in terms of the dimer model: the coupling constants associated with the modulation of the intra-dimer hopping integral are assumed independent of k , whereas the inter-dimer's are assumed to have the following dependence: $g(k; k^0; j) = \sum_R g_{KL}(qj) (e^{ik^0 R} - e^{ik R})$, where $q = k^0 - k$, and R represents the nearest neighbor lattice vectors. For what concerns the q dependence, the optical modes are taken independent of q , whereas for acoustic phonons we have simply assumed $g_{KL}(qj) / j q j$ up to the average value calculated at the zone edges.

Fig. 2 shows the frequency dispersion of the acoustic modes along representative Brillouin zone directions, together with a pictorial representation of the coupling strength at the zone edges. The dots diameters are proportional to the squared coupling constant, which are much larger along the Y , Z directions (i.e. the b , c axes) than along the diagonal. Our results indicate that for $-(BEDT-TTF)_2I_3$ the coupling of acoustic phonons is very anisotropic.

From the coupling constants in reciprocal space and the QHLD phonon density of states we calculate the Eliashberg coupling function [13]: $\sum_j h_{jF}^2(k; k^0; j) f_j(\omega_{qj}) \Gamma_{Fj}$, where $N(\Gamma_F)$ is the unit cell density of states/spin at the Fermi level, and h_{jF} indicate the average over the Fermi surface. Fig. 3 compares $-(BEDT-TTF)_2I_3$ Eliashberg functions. Both curves have been smoothed by a Gaussian of constant width to ease the comparison. Although significant differences exist, also due to the higher number

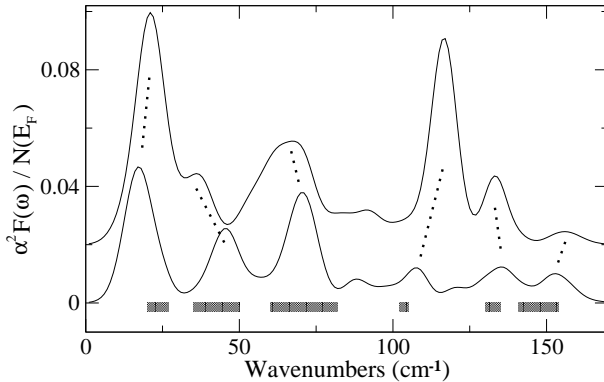


FIG. 3: Calculated Eliashberg function of $-(\text{BEDT-TTF})_2\text{I}_3$ (lower curve) and $-(\text{BEDT-TTF})_2\text{I}_3$ (upper curve, o set for clarity). The shaded areas at the bottom indicate the position of the most strongly coupled phonons, as detected from Raman and others phase BEDT-TTF salts (from Ref. 4).

of phonons for the α -phase unit cell, the most significant peaks are correlated, as indicated by the dotted lines. In both salts the lowest frequency peak results from the overlap of acoustic and lowest frequency optical modes.

Comparison of the computed Eliashberg function with available experimental data provides a test for the e-EP constants and QHLD eigenvectors. For the α -phase, the calculation compares quite favorably [7] with the Eliashberg function directly derived from point contact measurements. This kind of measurement is not available for $-(\text{BEDT-TTF})_2\text{I}_3$, but we can make reference to the phonon self-energy effects measured by Raman on $-(\text{BEDT-TTF})_2\text{Cu}(\text{NCS})_2$ and $-(\text{BEDT-TTF})_2\text{Cu}(\text{CN})_2\text{Br}$ [4]. A quantitative comparison is not possible, due to the different counter-ions. Nevertheless, Fig. 3 shows that the frequency regions (shaded areas at the bottom) of the few strongly coupled optical phonons [4], indeed correspond to the peaks of $-(\text{BEDT-TTF})_2\text{I}_3$ Eliashberg function. We finally mention that inelastic neutron scattering on $-(\text{BEDT-TTF})_2\text{Cu}(\text{NCS})_2$ [5] evidences also the involvement of acoustic phonons, in agreement with our findings.

Although further measurements, like Raman spectra with excitation in the infrared, are highly desirable to provide further tests, we believe that the above comparison already gives confidence to the QHLD eigenvectors, and as an example we show in Fig. 4 the eigenvector corresponding to $-(\text{BEDT-TTF})_2\text{I}_3$ zone edge acoustic phonon at 21 cm^{-1} . As it occurs in several other cases, the coupling is induced by the relative displacement of BEDT-TTF along the long molecular axis, i.e. roughly normal to the BEDT-TTF layers. Moreover, a normal mode coupled to electron is in general a mixture of both BEDT-TTF and I_3 vibrations. This mode mixing indicates that also the counter-ion vibrations may play an indirect role in the coupling.

We now proceed to estimate the critical temperatures.

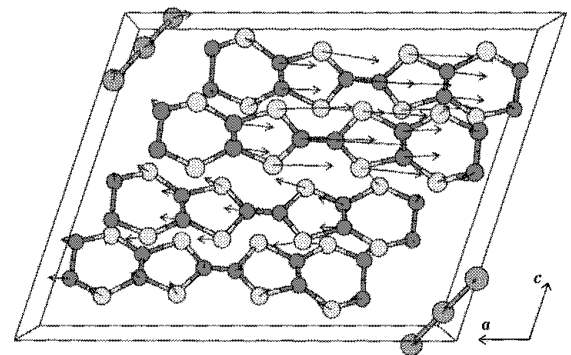


FIG. 4: Eigenvector of $-(\text{BEDT-TTF})_2\text{I}_3$ zone edge (Y) acoustic phonon at 21 cm^{-1} .

From Fig. 3 Eliashberg function we derive the dimensionless coupling constant $\text{!}_{\text{in}}^{\text{LP}}$, and the logarithmic average frequency $\text{!}_{\text{in}}^{\text{LP}}$ [13]:

$$\text{!}_{\text{in}}^{\text{LP}} = 2 \sum_0^{\text{R}_{\text{!max}}} \frac{\sum_{\text{!}}^2 \text{F}(\text{!})}{\text{!}} \text{d}! \quad (2)$$

$$\text{!}_{\text{in}}^{\text{LP}} = \exp \frac{2}{\text{!}_{\text{in}}^{\text{LP}}} \sum_0^{\text{R}_{\text{!max}}} \frac{\sum_{\text{!}}^2 \text{F}(\text{!})}{\text{!}} \ln \text{!} \text{d}! \quad (3)$$

The value depends on $N(E_F)$. With our tight binding EH calculation we estimate $N(E_F) = 5.4$ and 3.8 spin states/eV unit cell, so that $\text{!}_{\text{in}}^{\text{LP}} = 0.59$ and 0.65 for α - and $-(\text{BEDT-TTF})_2\text{I}_3$, respectively. The corresponding $\text{!}_{\text{in}}^{\text{LP}}$ values are 27 and 40 cm^{-1} . When these values are inserted into the Allen-McMillan equation [13]:

$$T_c = \frac{\text{!}_{\text{in}}}{12} \exp \frac{1.04(1 + \text{!}_{\text{in}})}{(1 + 0.62)} ; \quad (4)$$

assuming the standard 0.1 value for the Coulomb pseudopotential !_{in} , one obtains $T_c = 0.8$ and 1.7 K for α - and $-(\text{BEDT-TTF})_2\text{I}_3$, respectively, to be compared with the experimental values of 3.4 and 8.1 K [7, 10]. Of course, the T_c values depends critically on $N(E_F)$, a parameter difficult to evaluate [14]. However, even by taking the maximum current estimates, derived from experiment and therefore enhanced by many body electron-electron and electron-phonon effects [14], the T_c values (2.7 and 3.6 K) remain significantly below the experiment. Therefore e-EP coupling alone cannot reasonably account for the T_c of the two salts.

However, one must not forget high frequency e-MV coupled phonons [6, 15]. By including these phonons into the calculation of !_{in} , the above scenario changes substantially. We underline that e-MV coupling gives an additive contribution to the total $\text{!}_{\text{in}} = \text{!}_{\text{in}}^{\text{LP}} + \text{!}_{\text{in}}^{\text{MV}}$, whereas the contribution to $\text{!}_{\text{in}}^{\text{LP}}$ is multiplicative: $\text{!}_{\text{in}}^{\text{LP}} = \text{!}_{\text{in}}^{\text{LP}} \text{!}_{\text{in}}^{\text{MV}}$, where $\text{!}_{\text{in}}^{\text{MV}} = \exp \frac{2N(E_F)}{N} \frac{g_1^2}{1 + g_1^2} \ln \text{!}_{\text{in}}$, with g_1 the e-MV coupling constants and N the number of molecules per unit cell [15]. It turns out that by including the e-MV coupling, T_c increases by only 25% ,

but λ_{ln} reaches 60 and 94 cm⁻¹ for - and -(BEDT-TTF)₂I₃, respectively. By using these new values into Eq. (3), keeping $\gamma = 0.1$, we find that our tight binding EH N (E_F) estimates, which are within the range of the currently accepted values [14], account for the observed critical temperatures. In particular, precise T_c matching requires N (E_F) = 5.2 and 3.9 spin states/(eV unit cell), corresponding to a total of 0.74 and 0.91 for - and -(BEDT-TTF)₂I₃, respectively. We finally remark that only by using the new λ_{ln} , which does not depend on N (E_F), the empirical relation [16] connecting this parameter to the specific heat jump C_p = T_c yields for -(BEDT-TTF)₂I₃ a jump in nice agreement with experiment (1.7 vs 1.6) [10].

In our approach electron-phonon coupling provides a consistent and plausible explanation of many experimental findings related to the superconducting properties of - and -phase BEDT-TTF salts. Besides the just mentioned T_c values and specific heat jump, the scattered experimental evidences of the involvement of acoustic and optical lattice phonons have been rationalized. The coupling of acoustic phonons in the -phase turns out to be strongly anisotropic, likely yielding an anisotropic gap that might confuse the node search [17]. In addition, we have found that the most strongly e-LP coupled BEDT-TTF modes in π planes approximately normal to the conducting planes, with counter-ions vibrations fixed to BEDT-TTF ones (cf. Fig. 4). This finding might well account for the "interlayer effects" detected in thermal expansion measurements [18]. Experimental evidences in favor of the involvement of e-M V coupled phonons are mainly related to isotopic effects [3, 19]. In particular, the universal inverse deuterium isotope effect (0.25 K) is likely due to a small increase in λ_{ln} . The e-M V coupling constants of deuterated BEDT-TTF are not known, but we have verified that very small and plausible changes of the coupling constants with respect to those of pristine BEDT-TTF [6] may indeed lead to the required increase in T_c, despite the large downwards shift of several frequencies upon deuteration.

The principal conclusion of our paper is that phonons are the main responsible for the coupling mechanism in BEDT-TTF based oSC. The role of phonons is complex, or "entangled", in the sense that different kinds of phonons are all important, but contribute in different ways. The acoustic and optical lattice phonons, modulating t, give the main weight to λ_{ln} , but intramolecular phonons modulating on-site energies are essential in increasing the average λ_{ln} value. Although here we vindicate the role of phonons, we also stress that traditional phonon mediated pairing alone cannot give reason of all the experimental findings related to superconducting properties of BEDT-TTF salts. The proximity of antiferromagnetic or charge ordered states in many oSC clearly indicate that electron-electron interactions are important [1], and these cannot be properly accounted for in our

effective single particle approach. In particular, just consider the above mentioned -(BEDT-TTF)₂Cu(NCS)₂ and -(BEDT-TTF)₂Cu(NCN)₂Br salts. Their λ_{ln} is similar to -(BEDT-TTF)₂I₃, yet their T_c's are 9.5 and 11.5 K, respectively [20]. We think it is unlikely that the corresponding increase in λ_{ln} with respect to -(BEDT-TTF)₂I₃ can be attributed to a significant change in the e-LP coupling strength due to the change in counter-ions. Rather, we believe that electron-electron interactions and/or the proximity of a phase boundary may lead to an enhancement of the effective electron-phonon coupling. In other words, we need to analyze the role of electron-phonon coupling in low-dimensional strongly correlated materials, still a poorly understood topic [21]. Our work represents the necessary prerequisite for such an analysis in BEDT-TTF-based oSC.

Work supported by the Italian Ministero Istruzione, Università e Ricerca (M.I.U.R.). We thank L. Frediani for the DFT calculations, and A. Painelli for discussions.

- [1] J. Wosnitza, *Curr. Op. Solid State Mater. Science*, 5, 131 (2001); J. Singleton, *Rep. Progr. Phys.* 63, 1111 (2000).
- [2] J. Schmalian, *Phys. Rev. Lett.* 81, 4232 (1998); J. M. Erino and R. H. M. Kenzie, *Phys. Rev. Lett.* 87, 237002 (2001).
- [3] V. M. Erzhanov et al., *C. R. Acad. Sci. Paris*, 314, 563 (1992).
- [4] D. Pedron et al., *Physica C* 276, 1 (1998); E. Falques et al., *Phys. Rev. B* 62, R 9291 (2000); D. Pedron et al., *Synth. Metals* 103, 2220 (1999).
- [5] L. Pintschovius et al., *Europhys. Lett.* 37, 627 (1997).
- [6] G. V. Isentini et al., *Phys. Rev. B* 58, 9460 (1998), and references therein.
- [7] A. G. Orlando et al., *Phys. Rev. B* 62, 14476 (2000).
- [8] A. Brillante et al., *Chem. Phys. Lett.* 274, 478 (1997); R. G. Della Valle et al., *Physica B*, 265, 195 (1999).
- [9] H. K. Obayashi et al., *J. Mater. Chem.* 5, 1681 (1995).
- [10] J. Wosnitza et al., *Phys. Rev. B* 50, 12747 (1994).
- [11] The t values are available on request. See also A. Fortunelli and A. Painelli, *Phys. Rev. B* 55, 16088 (1997).
- [12] G. V. Isentini et al., *Europhys. Lett.* 42, 467 (1998).
- [13] P. B. Allen and R. C. Dynes, *Phys. Rev. B* 12, 905 (1975).
- [14] J. M. Erino and R. H. M. Kenzie, *Phys. Rev. B* 62, 2416 (2000) and references therein.
- [15] D. Pedron et al., *Mol. Cryst. Liq. Cryst.* 234, 161 (1993).
- [16] F. M. Marsiglio and J. P. Carbotte, *Phys. Rev. B* 33, 6141 (1986).
- [17] There is no agreement yet about the gap symmetry. The following studies on -(BEDT-TTF)₂Cu(NCS)₂ are in favor of s, d_{xy}, and d_{x²-y²} symmetry, respectively: J. M. Uller et al., *Phys. Rev. B* 65, 140509 (2002); K. Iwasa et al., *Phys. Rev. Lett.* 86, 2653 (2001); T. Arai et al., *Phys. Rev. B* 63, 104518 (2001). See also: G. Varelogiannis, *Phys. Rev. Lett.* 88, 117005 (2002).
- [18] J. M. Uller et al., *Phys. Rev. B* 65, 144521 (2002).
- [19] J. A. Schlueter et al., *Physica C* 351, 261 (2001).
- [20] H. Eisinger et al., *Phys. Rev. Lett.* 84, 6098 (2000).
- [21] A. Lanzara et al., *Nature* 412, 510 (2001).